

Structural Properties of Fractionated Starch Polymers and Their Dependence on the Dissolution Process

R. Hanselmann and W. Burchard*

Institut für Makromolekulare Chemie, Albert Ludwigs Universität Freiburg, SonnenStrasse 5, 79104 Freiburg i. Br., Germany

M. Ehrat and H. M. Widmer

CIBA GEIGY AG, Corporate Analytical Research, CH-4002 Basel, Switzerland

Received September 25, 1995; Revised Manuscript Received January 16, 1996

ABSTRACT: A combination of sedimentation field flow fractionation (SdFFF) with multiangle laser light scattering (MALLS) was applied to the grain level destructured potato and waxy corn starch in solution. The molar mass and radius distributions were obtained simultaneously. Separation was observed for a radii range of 50–500 nm. Degradation upon heat exposure was found depending mainly on the exposure time and less on the temperature. A detailed analysis of the particle scattering factors (angular dependence of the scattered light) revealed small differences in the internal structure of potato and waxy corn starches. Both starches showed the behavior of only weakly swollen, branched clusters. Potato starch appeared to be slightly more expanded than waxy corn starch. Self-similar structures were observed with fractal dimensions of 2.4 ± 0.1 . The deviations from theoretical predictions using the mean field approximation could result from excluded volume effects and heterogeneity in branching.

Introduction

Starch is one of the most abundant polysaccharides in nature. It is a cheap raw material and therefore of high economic importance. Native starch of different origins contains the branched amylopectin and the linear amylose in various ratios, which range from 0% up to about 70% amylose.^{1–3} Molar masses of 10^5 to 10^6 Da were reported for amylose. Amylopectin, however, has a much larger weight average molar mass in the range 10^7 and 10^8 Da.^{2,3} Native starch is deposited in the form of partially crystalline granules. In order to dissolve this material in water, the granules have to be destructured under drastic conditions without degrading the macromolecular structure. These optimum conditions had to be found by varying the temperature and the duration of heat exposure. Molecularly dispersed solutions can be obtained by heating the granule suspensions under autoclaving conditions to temperatures higher than 135 °C.^{3–6} The presence of linear amylose and branched amylopectin molecules in solution and the resulting high polydispersity make it difficult to derive reliable information on the structural properties of each type of particle by common physical techniques of measurement.³ Characterization by common analytical size exclusion chromatography (SEC) fails because of the ultrahigh molar masses of amylopectin.

Recently, we reported on molar mass distributions which were obtained by sedimentation field flow fractionation (SdFFF).⁶ SdFFF is a pseudochromatographic separation method⁷ and allows separation of particles according to their hydrodynamic volume and density. The separation of particles is induced by a gravitational field oriented perpendicularly to the flow direction. The detection of the eluted fractions was performed on-line with a multiangle laser light scattering (MALLS) photometer and an interferometric refractometer. The combination of the on-line light scattering detection with this fractionation method allowed determination of the molar mass and the radius of gyration of the investi-

gated sample in each eluted volume element. With these data the distribution of both, the molar mass and the radius of gyration, were established. A satisfactory separation into fractions was obtained, even for molar masses larger than 10^9 Da.

In the above mentioned paper⁶ the SdFFF technique was introduced and the high efficiency of the method was demonstrated with two starches of different amylose contents as examples. In this paper we report on the determination of the structure of the various fractions of the same samples, as discussed in ref 6 by quantitative evaluation of the angular dependence of the scattered light, that defines the particle scattering factor $P(q)$. Each particle scattering function corresponds to a small slice in the distribution which contains a polymer fraction of low polydispersity. The analysis of the obtained particle scattering factors allowed extraction of information on the structural properties of amylopectin particles from one starch sample as a function of their molar mass. It also allowed comparison of structures of amylopectin particles from different sources. In fact, the application of SdFFF/MALLS led to information which is not accessible by other commonly applied analytic methods.

Experimental Section

Sample Preparation. A potato and a waxy corn starch were investigated. They were dissolved under different conditions in a 0.05% (w/v) sodium azide solution. (to prevent bacterial growth). The waxy corn starch samples were heated at 175 °C for different periods of time (20, 40, and 60 min). The potato starch samples were heated for 40 min but at different temperatures (160, 170, and 175 °C). Concentrations between 1 and 5 mg/mL were chosen. In all cases clear solutions were obtained. Further details were given in paper I.⁶

SdFFF/MALLS.^{8–10} The differently treated samples were fractionated by SdFFF/MALLS.

An automated SdFFF based on the "SF³ 1000 Particle Fractionator" (DuPont Instruments)^{11,12} was used. The light scattering detection was performed with the DAWN F laser photometer (Wyatt Technology), whereas for the detection of the concentration, the Optilab 903 interferometric refractometer (Wyatt Technology) was used.

* Abstract published in *Advance ACS Abstracts*, April 1, 1996.

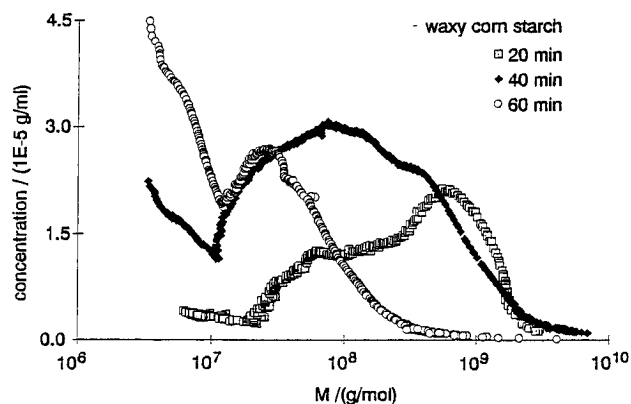


Figure 1. Molecular weight distributions of waxy corn starch treated at 175 °C for different periods of time.

Table 1. Molecular Characteristics of a Waxy Corn Starch after Heat Treatment at 175 °C for 20, 40, and 60 min (d_f = Fractal Dimension, C = Fitting Parameter According to Eq 2)

heating period (min)	$10^{-6}M_w$ (Da)	$10^{-6}M_n$ (Da)	M_w/M_n	R_g (nm)	d_f	C
20	360.0	43.0	8.2	320	2.39	0.0228
40	167.0	20.8	8.0	272	2.45	0.0158
60	37.5	12.5	3.0	121	2.49	0.0079

Table 2. Molecular Characteristics of a Potato Starch after a Heat Treatment for 40 min at 160, 170, and 175 °C (Symbols as in Table 1)

heating temp °C	$10^{-6}M_w$ (Da)	$10^{-6}M_n$ (Da)	M_w/M_n	R_g (nm)	d_f	C
160	353.9	46.8	7.6	305	2.30	0.0276
170	67.1	13.7	4.9	212	2.35	0.0211
175	56.4	13.8	4.1	199	2.36	0.0210

A comprehensive description of the instrumental setup and the measuring conditions were published previously in paper I.⁶ Here we repeat only the information necessary for instrumental reasons since the measurements were difficult.

Results

Molar Mass Dependence of the Radii of Gyration. Starch molecules (amylopectin) in the range of R_g from 50 to 500 nm could be analyzed by the SdFFF technique. The fraction of particles smaller than 50 nm in size were not retained and were eluted unfractionated in the so-called void peak. The mass fraction of unretained polymer ranged from 3% to 25% depending on the heating conditions, i.e., temperature and time of exposure, respectively. Therefore, the recorded radius and molar mass distributions represent only 97% to 75% of the total amount of injected polymer. Thus, the calculated averages of the molar mass and the radius of gyration as given in Tables 1 and 2 are subject to this error. In Figure 1 the molar mass distributions of the three differently treated waxy corn starches are shown. They were heated at 175 °C for 20, 40, and 60 min, respectively. Figure 2 exhibits the corresponding distributions of the three potato starches heated for 40 min at 160, 170, and 175 °C, respectively. These different autoclaving conditions were applied to obtain an insight on the effect of temperature and the time of exposure. The average molar masses and radii of gyration were found to shift to lower values when the heating period or the heating temperature were increased during the dissolution process. The observed behavior has been interpreted to be due to two effects. The first is the presence of aggregates which are broken up on heating.

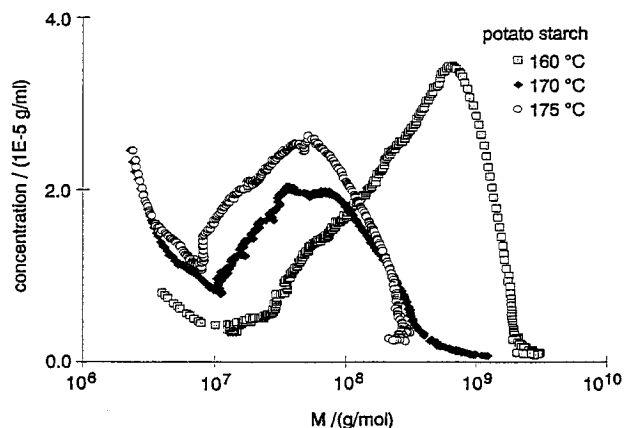


Figure 2. Molecular weight distributions of three samples of potato starch dissolved at different temperatures.

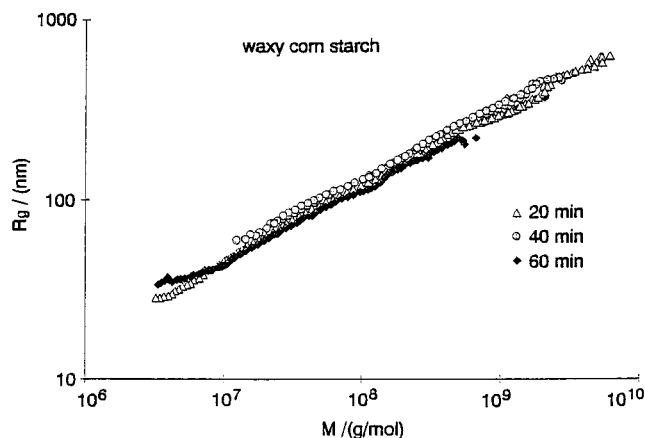


Figure 3. Molecular weight dependences of the radii of waxy corn starch treated for different periods of time.

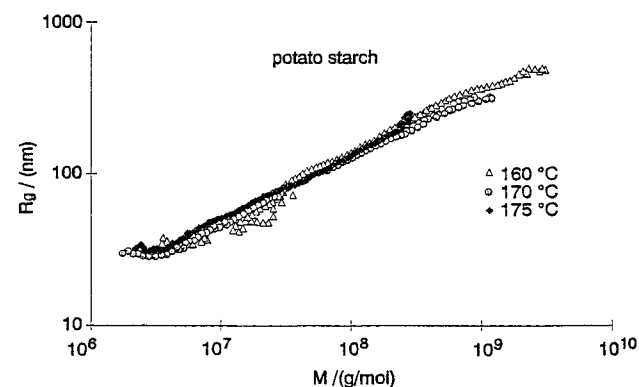


Figure 4. Radius-molecular weight correlation of three potato starch samples treated for 40 min at different temperatures.

The second effect is degradation of the polymer (breaking of covalent bonds) in the harsh dissolution process.

Figure 3 shows the molar mass dependences of the radius of gyration from the three differently treated waxy corn starches. Within the limit of experimental error the R_g - M relationship follows a common straight line in the double logarithmic plot and can be described by the power law behavior $R_g = KM^\nu$ with $\nu = 0.41 \pm 0.01$. Similar behavior was found for potato starch (Figure 4) with $\nu = 0.42 \pm 0.01$. Here we disregarded the molar masses larger than 10^9 which due to the large scattering of data would make the slope more uncertain. Measurements of such high molar masses with radii of gyration larger than 300 nm are extremely difficult to measure accurately. Furthermore these high values of

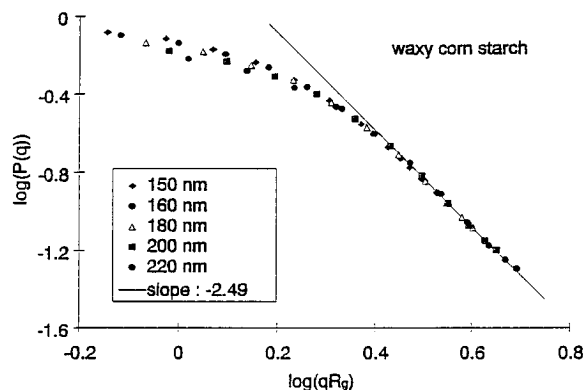


Figure 5. Double logarithmic plot of five particle scattering factors vs the normalized scattering vector. The scattering factors relate to five different slices of the molecular weight distribution of the 60 min heated waxy corn starch.

M and R_g may also arise from aggregates which probably have fractal dimensions d_f larger than 2.4 or smaller values for ν ($\nu < 0.41$).

Particle Scattering Factor. Further information about the structure of polymers can be obtained from the particle scattering factor $P(q)$, which describes the angular distribution of the scattered light. For a preliminary analysis, the scattering intensity $(R(\theta)/Kc)$ or the corresponding particle structure factor $P(q) = R(\theta)/R(\theta=0)$ was plotted against the value of the scattering vector q in a double logarithmic scale, where $q = (4\pi/\lambda) \sin(\theta/2)$, with λ the wavelength of the light in the solution and θ the scattering angle. For large particles a straight line with a negative slope at large q was obtained, but for the smaller particles this asymptote was not reached, since the experimentally accessible q range remained too small. However, the various curves could be contracted into one master curve, when $P(q)$ was plotted against qR_g , where $R_g \equiv \langle s^2 \rangle_z^{0.5}$ is the radius of gyration of the different samples. Such a master curve is expected for "self-similar" structures which will be defined below in the Discussion.

In Figure 5 the particle scattering factors from five different fractions of the waxy corn starch sample, heated for 60 min, are plotted against the dimensionless parameter $u (=qR_g)$. The scattering factors correspond to starch molecules from five different slices of the distribution and have therefore different radii of gyration. One common curve is indeed obtained, and at $\log(qR_g) > 0.4$ power law behavior is observed. The asymptotic slope of this curve is $-d_f = -2.43 \pm 0.05$. Very similar behavior was found for waxy corn and potato starches, independent of the kind of treatment, but the derived exponents $d_f = 2.36 \pm 0.03$ (Tables 1 and 2) differ slightly. They show dependence on the type of starch as well as on the kind of treatment. The exponent d_f of waxy corn starch increases with elongated heating period. For potato starch, dissolved at 160 °C, the exponents d_f are lower than those of the same potato starches treated at higher temperatures. The difference in d_f between the two samples treated at 170 and 175 °C is negligible.

Additional information was obtained when the particle scattering factor was plotted in a Kratky plot¹³ ($u^2P(q)$ vs u). In this kind of diagram the asymptotic region at high u values is given increasing weight. Therefore, even small changes in the particle scattering factor in this u domain can be detected and these are related to the internal structure.¹⁴ In Figure 6 the particle scattering factors (obtained from particles with

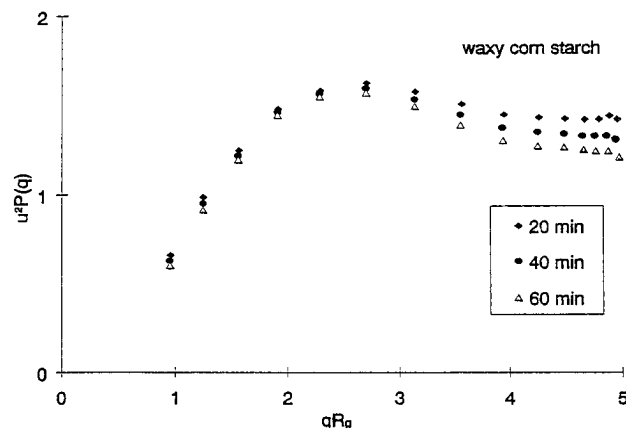


Figure 6. Kratky plot of the three different waxy corn starches. The particle scattering functions were obtained from particles with a 200 nm radius.

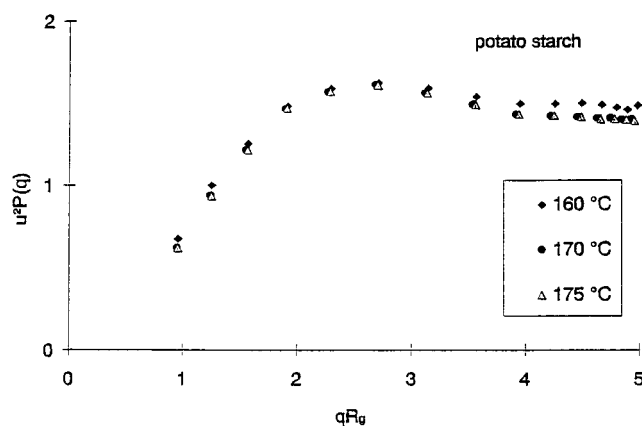


Figure 7. Same Kratky diagram as in Figure 6 for the three potato starches.

$R_g = 200$ nm) of the three differently treated waxy corn starches are plotted in such a Kratky diagram. The three functions agree well at $u = qR_g < 2.5$ but differ in the asymptotic region. The longer the heating period of the sample the stronger the function decreased as u became large. Each of the three functions have a maximum close to $u = 2.5$, which was predicted for branched polymers of the amylopectin type¹⁵ by applying the technique of cascade theory developed by Gordon.¹⁶ In Figure 7 the same plot as in Figure 6 is shown for the three potato starch samples. The particle scattering functions of the starches treated at 170 and 175 °C display no significant deviations, whereas the function of the sample dissolved at 160 °C exhibits a slightly different shape at high u values.

Discussion

The experimental data obtained by the SdFFF technique revealed three striking features:

(i) Power law behavior is obtained for the radius of gyration as a function of the particle mass with exponents of $\nu = 0.41 \pm 0.01$ and 0.42 ± 0.01 for waxy corn and potato starch, respectively. The curves of the two starches deviate only slightly from each other but show no variation with the stage of degradation due to the heat treatment.

(ii) An asymptotic power law behavior is found for the angular dependence of the particle structure factor $P(q)$ with exponents of $d_f = 2.43 \pm 0.05$ and $d_f = 2.35 \pm 0.03$ for the two starches from corn and potato, respectively.

(iii) A common master curve for the particle structure factor as a function of qR_g is found that only slightly deviates in the high qR_g range for the various starches.

These results are clear indications for self-similar structures, now frequently called fractals. Another point of interest are the small deviations from the master curve at large qR_g , which nevertheless are significant and characteristic of the type of starch.

Self-Similarities and Fractal Behavior. The molar mass dependence of the radius of gyration can be rewritten as a power law of the molar mass.

$$M = K' R_g^{1/\nu} = K' R_g^{d_f} \quad (1)$$

Such a relationship can formally be considered as a definition of a dimension. For instance $d = 3$ would define a globular homogeneous structure, and $d = 2$ or 1, planar and linear structures, respectively. With the values of $\nu = 0.41$ and 0.42 one obtains $d_f = 2.44$ and 2.38 which are no longer integers but fractal dimensions. Such fractal dimensions are common for disordered objects and demonstrate self-similarity behavior.¹⁷ The latter is understood as a structure that independently of a length scale displays the same behavior. In other words, if two pieces of different sizes are cut from the particle and the smaller is optically magnified to equal size, then the structures appear indistinguishable. The observed self-similarity of these correlated branch structures is not a trivial result and was not really expected. We had no prior estimate of the spatial length on which the correlated reaction occurs, but self-similarity can only be found when this correlation length is much smaller than the length scale that is observed by static light scattering. A fractal dimension of 2.44 is characteristic of a particle that has an internal structure between a hard sphere ($d_f = 3.0$) and a fully swollen randomly branched macromolecule in a thermodynamically good solvent ($d_f = 2.0$).^{18,19} A fractal dimension of $d_f = 2.5$ is predicted for branched clusters which are not swollen,¹⁸ either for thermodynamic reasons (Θ -conditions) or because of steric hindrances.

Thus we conclude that the starches are only weakly swollen in water at 20 °C and that potato starch can swell to a slightly larger extent than waxy corn starch.

These results are confirmed by the slope of the scattering intensity as a function of the scattering vector q in the double logarithmic plot. The theory of fractals interprets this slope again as being a fractal dimension. In the latter experiment d_f is found from the *internal* structure in contrast to eq 1 that is related to the *global* structure.¹⁸

In percolation theory (site or bond percolation) two types of fractal dimensions are distinguished. The first one $d_{f(\text{app})}$ comprises the whole system and corresponds to an average over all cluster sizes. It is obtained experimentally from (i) the angular dependence of the scattered light and (ii) from the exponent in eq 1. More interesting, however, is the fractal dimension of the individual clusters d_f , which is obtained from $d_{f(\text{app})}$ by a polydispersity correction. For random branching or aggregation processes the following relationship is found

$$d_f = d_{f(\text{app})}/(3 - \tau) \quad (2)$$

where $\tau = 2.2$ is the exponent in the molar mass distribution

$$w(M) = AM^{1-\tau} \exp(-M/M_z) \quad (3)$$

with M_z the z -average of the molar mass. The distribu-

tion (3) has the property that $M_w/M_n \sim M_w$ and $M_z/M_w \sim M_w^{0.25}$; i.e., both ratios increase with M_w and diverge at the gel point. No correction for polydispersity is needed for Schulz–Zimm types of distributions, since here the polydispersity ratios M_w/M_n and M_z/M_w do not depend on the molar mass. In such cases we have

$$d_f = d_{f(\text{app})} \quad (4)$$

The molar mass distributions of the three fractions obtained from the original system are not fully known, but the data we could measure so far clearly demonstrate no power law behavior of the type given in eq 3. Instead, the distributions resemble the Schulz–Zimm type. The amylopectin structure belongs to the class of hyperbranched macromolecules and is the result of a correlated reaction. In terms of the three reactive OH groups in the C₁ (A), C₄ (B), and C₆ (C) positions of the glucose monomer, this means group A can react only with group B or group C. This hyperbranched structure was previously denoted as the ABC model and was theoretically treated by French and Erlander²⁴ and by one of the present authors (W.B.).¹⁵ French and Erlander derived also the mass fraction of the molar mass distribution, which indeed displays the relation to the Schulz–Zimm type. The first three moments are related to the M_n , M_w , and M_z averages. The polydispersity index M_w/M_n grows asymptotically with $M_w^{0.5}$, but the other polydispersity index M_w/M_z approaches a constant value of 3. When the apparent fractal dimension is corrected for polydispersity the M_w/M_z ratio has to be used, but this ratio is small and almost constant, in contrast to the behavior of randomly branched macromolecules. Hence, for a correlated reaction that leads to the hyperbranched structures, the apparent fractal dimension is practically indistinguishable from the fractal dimension of individual clusters, $d_{f(\text{app})} \cong d_f$.

Particle Structure Factor. Because of the self-similarity characteristics demonstrated by the radius of gyration, the common master curve for $P(q)$ as a function of qR_g offers no surprise. (Here the scaling parameter for q is the radius of gyration.) A closer look at the asymptotic qR_g region reveals, however, small variations which are clearly outside the margins of experimental error and demonstrates therefore structural differences.

When these small differences are neglected, it turns out that the curves for the nonfractionated waxy corn and potato starches in the Kratky representation are very satisfactorily described by the following equation¹⁵

$$u^2 P_z(q) = u^2 (1 + C(u^2/3)) / [1 + (1 + C)(u^2/6)]^2 \quad (5)$$

with C parameters as given in Tables 1 and 2. Equation 5 has been theoretically derived from the already mentioned so-called ABC-polycondensation process with the constraints that only the functional groups B and C (OH in the C₄ and C₆ positions) can react with group A (reducing end group in the C₁ position).^{15,20} The reactivity of the C₆ group defines the degree of branching,¹⁴ and this branching density is again related to the C parameter in eq 5³ (a low C parameter indicates high branching density, and $C = 1$, a linear structure).

One notices that treatments at different temperatures but identical time intervals did not cause a change in the branching density of potato starch, although the average particle mass was decreased at higher temperatures. In contrast, the exposure times at high temperatures changed the C parameter for the waxy corn

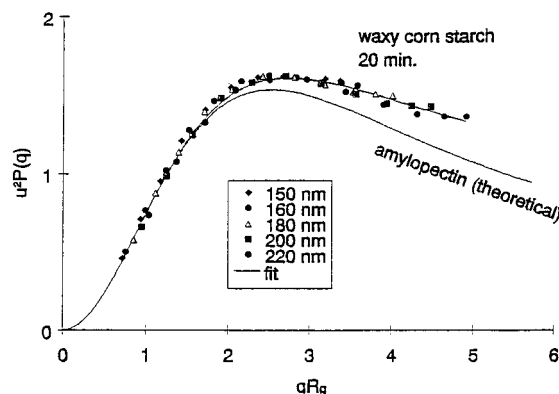


Figure 8. Kratky plot of five particle scattering functions each obtained from an other slice of the molecular weight distribution of the 20 min heated waxy corn starch. Additionally, the fit through the data and the theoretically calculated relationship were illustrated.

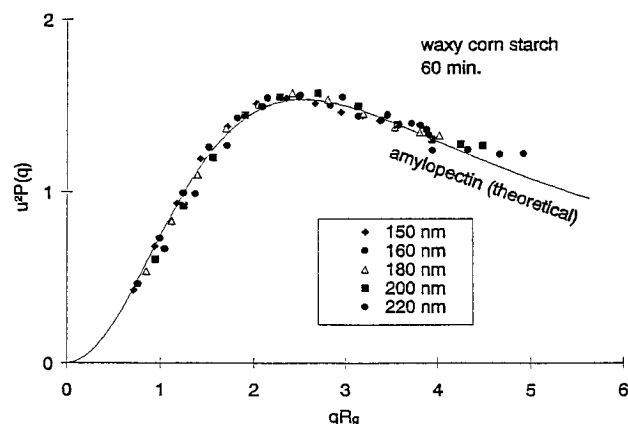


Figure 9. Kratky plot of five particle scattering functions each obtained from an other slice of the molecular weight distribution of the 60 min heated waxy corn starch. Additionally, the fit through the data and the theoretically calculated relationship were illustrated.

starch significantly, indicating higher branching densities. Simultaneously, a strong degradation was observed.

Two conclusions can be drawn from these effects. One is that mainly the duration of temperature exposure causes a change in the internal structure, and the second is that the degradation results in a higher branching density. This effect can be explained by the heterogeneous branching structure in the starch molecule and by a degradation occurring preferentially in the weakly branched domains. Heterogeneous branching has been inferred previously from enzymatic degradation²¹ and morphology studies on starch granules.²²

Finally, the scattering curves from five slices of the distributions are compared (Figures 8–11). These curves show the striking difference from the unfractionated samples of a continuous decrease at large qR_g , while the nonfractionated samples exhibit a slight increase. In a previous paper Aberle et al.³ interpreted this increase as an effect of the presence of linear amylose chains. The present experimental findings now demonstrate that the amylose content cannot be the only reason, since waxy corn starch contains no amylose, but nevertheless, the unfractionated sample displays this increase,³ whereas the curves of the different waxy corn starch fraction slices decrease (see Figure 6). Possibly, the effect results from a fraction of degraded material, which indeed would cause a similar behavior

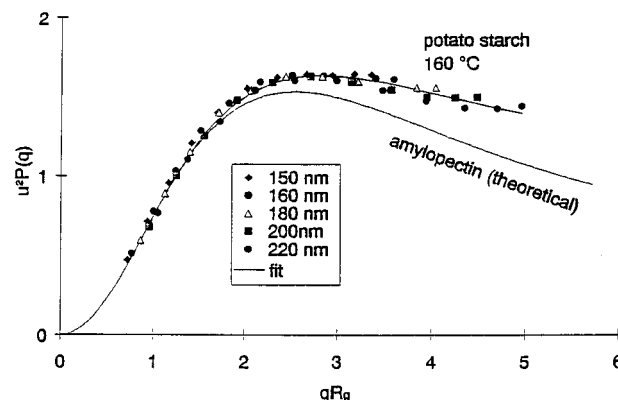


Figure 10. Kratky plot of five particle scattering functions each obtained from an other slice of the molecular weight distribution of the potato starch heated at 160 °C. Additionally, the fit through the data and the theoretically calculated relationship were illustrated.

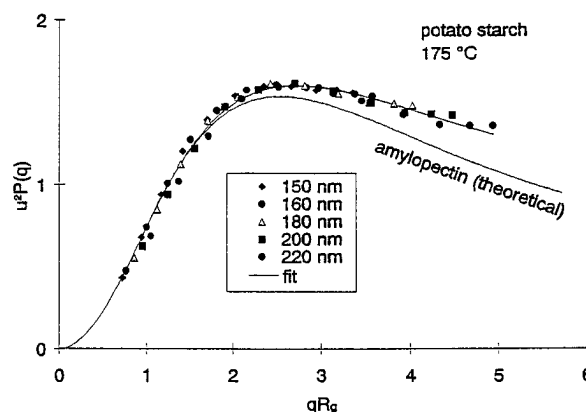


Figure 11. Kratky plot of five particle scattering functions each obtained from an other slice of the molecular weight distribution of the potato starch heated at 175 °C. Additionally, the fit through the data and the theoretically calculated relationship were illustrated.

independent of whether this low molar mass fraction is linear or branched.

An interpretation in terms of a bimodal distribution is in agreement with the smoothly decreasing asymptote for the monodisperse fractions. For comparison in Figures 8–11 the theoretical curve with $C = 0.0076^{3,14}$ is shown as a full line. This curve corresponds to the homogeneously branched amylopectine. The deviations can be interpreted as the result of the heterogeneous branching, but the same effect would also result from excluded volume interactions between the particles. The slightly more expanded swelling of potato starch agrees with the weaker asymptotic decay of $P(q) u^2$ at large qR_g , i.e., with a stronger excluded volume effect. ³¹P-NMR as well as H-NMR investigations have shown that, in contrast to waxy corn starch, 0.5% of the glucose units of potato starch are substituted with phosphate ester groups.²³ The repulsive forces of the equal charged phosphate ester groups are probably responsible for the higher swellability of the potato starch molecules in comparison to waxy corn starch.

Conclusion

Waxy corn and potato starch can be fractionated by the SdFFF technique within a range of R_g between 50 and 500 nm. The largest particles could be clusters of aggregated molecules, but such clusters would be difficult to distinguish from molecularly dispersed starch

molecules, since there is no detectable difference in the fractal dimensions. Both the aggregated clusters and the truly dissolved amylopectin molecules have similar fractal dimensions of $d_f = 2.4 \pm 0.1$ that exhibit low swellability. This effect is unexpected and may be interpreted by a structure that is stabilized and fixed by the formation of intramolecular H bonds.

The slight differences in the structure between waxy corn and potato starch are detectable.

References and Notes

- (1) Shannon, J. C.; Garwood, D. L. In *Starch*, 2nd ed.; Whistler, R. L., BeMiller, J. N., Paschall, E. F., Eds.; Academic Press: New York, London, 1985; Chapt. III.
- (2) Guilbot, A.; Mercier, Ch. In *The Polysaccharides*; Aspinall, G. O., Ed.; Academic Press: New York, London, 1985; Vol. 3, p 2.
- (3) Aberle, T.; Burchard, W.; Vorwerg, W.; Radosta, S. *Starch* **1994**, *46*, 329.
- (4) Young, A. H. In *Starch, Chemistry and Technology*, 2nd ed.; Whistler, R. L., BeMiller, J. N., Paschall, E. F., Eds.; Academic Press: New York, London, 1985; Chapter VIII.
- (5) Gidley, M. J.; Bulpin, P. *Macromolecules* **1989**, *22*, 342.
- (6) Hanselmann, R.; Ehrat, M.; Widmer, H. M. *Starch*, submitted for publication.
- (7) Giddings, J. C. *J. Chromatogr.* **1976**, *125*, 3.
- (8) Giddings, J. C. *J. Chem. Phys.* **1968**, *49*, 81.
- (9) Hovingh, M. E.; Thompson, G. H.; Giddings, J. C. *Anal. Chem.* **1970**, *42*, 195.
- (10) Giddings, J. C. *Sep. Sci. Technol.* **1978**, *13*, 241.
- (11) Kirkland, J. J.; Rementer, S. W.; Yau, W. W. *Anal. Chem.* **1981**, *53*, 1730.
- (12) Yau, W. W.; Kirkland, J. J. *Sep. Sci. Technol.* **1981**, *16*, 577.
- (13) Kratky, O.; Porod, G. *J. Colloid. Sci.* **1949**, *4*, 35.
- (14) Burchard, W. *Adv. Polym. Sci.* **1983**, *48*, 1.
- (15) Burchard, W. *Macromolecules* **1972**, *5*, 604.
- (16) Gordon, M. *Proc. R. Soc. London* **1962**, *A268*, 240.
- (17) Schaefer, D. W.; Martin, J. E.; Hurd, A. J.; Keefer, K. D. In *Physics of Finely Divided Matter*; Boccarda, N., Daoud, M., Eds.; Springer: Berlin, 1985.
- (18) Stauffer, D. *Introduction to Percolation Theory*; Taylor & Francis: London, Philadelphia, 1985.
- (19) Stauffer, D.; Coniglio, A.; Adam, M. *Adv. Polym. Sci.* **1982**, *44*, 103.
- (20) Flory, P. J. *Principles of Polymer Chemistry*; Cornell University Press: Ithaca, NY, 1953.
- (21) Robin, J. P.; Mercier, Ch.; Dubrat, F.; Charbonniere, R.; Guilbot, A. *Starch*, **1975**, *27*, 36.
- (22) Kainuma, K.; French, D. *Biopolymers* **1972**, *11*, 2241.
- (23) Wischmann, B.; Nielsen, T. H.; Bay Smidt, A. M.; Jacobsen, H. B.; Möller, B. L. Copenhagen, *Stärke Tagung* 1995.
- (24) Erlander, S.; French, D. *J. Polym. Sci.* **1956**, *20*, 7.

MA951452C